Extraordinarily Robust Polyproline Type I Peptoid Helices Generated via the Incorporation of α-Chiral Aromatic N -1-Naphthylethyl Side Chains

4 AUTHORS, INCLUDING:

J. Aaron Crapster
Stanford University
6 PUBLICATIONS **137** CITATIONS

SEE PROFILE

Ilia A Guzei
University of Wisconsin–Madison
340 PUBLICATIONS **6,696** CITATIONS

SEE PROFILE

Extraordinarily Robust Polyproline Type I Peptoid Helices Generated *via* the Incorporation of α-Chiral Aromatic *N*-1-Naphthylethyl Side Chains

Joseph R. Stringer, **J. Aaron Crapster**, **Ilia A. Guzei**, and **Helen E. Blackwell**[*]
Department of Chemistry, University of Wisconsin–Madison, 1101 University Avenue, Madison, WI 53706-1322

Abstract

Peptoids, or oligomers of *N*-substituted glycines, are a class of foldamers that have shown extraordinary functional potential since their inception nearly two decades ago. However, the generation of well-defined peptoid secondary structures remains a difficult task. This challenge is due, in part, to the lack of a thorough understanding of peptoid sequence-structure relationships and consequently, an incomplete understanding of the peptoid folding process. We seek to delineate sequence-structure relationships through the systematic study of noncovalent interactions in peptoids and the design of novel amide side chains capable of such interactions. Herein, we report the synthesis and detailed structural analysis of a series of (*S*)-*N*-(1-naphthylethyl)glycine (*N*s1npe) peptoid homooligomers by X-ray crystallography, NMR and circular dichroism (CD) spectroscopy. Four of these peptoids were found to adopt well-defined structures in the solid state, with dihedral angles similar to those observed in polyproline type I (PPI) peptide helices and in peptoids with α-chiral side chains. The X-ray crystal structure of a representative *N*s1npe tetramer revealed an all *cis*-amide helix, with approximately three residues per turn, and a helical pitch of approximately 6.0 Å. 2D-NMR analysis of the length-dependent *N*s1npe series showed that these peptoids have very high overall backbone amide $K_{cis/trans}$ values in acetonitrile, indicative of conformationally homogeneous structures in solution. Additionally, CD spectroscopy studies of the *N*s1npe homooligomers in acetonitrile and methanol revealed a striking length-dependent increase in ellipticity per amide. These *N*s1npe helices represent the most robust peptoid helices to be reported, and the incorporation of (*S*)-*N*-(1-naphthylethyl)glycines provides a new approach for the generation of stable helical structure in this important class of foldamers.

Introduction

The design and construction of synthetic foldamers capable of mimicking the structure and function of natural biopolymers is an active area of research.[1-3] The multitudinous functions performed by biological polymers such as proteins and RNA are made possible by the precise, three-dimensional arrangements of chemical functionality arising from distinct folds within their polymeric backbones. Thus, the ability to accurately and predictably assemble well-folded, higher order structures is paramount to understanding structure-function relationships within a particular foldameric class.

[*]To whom correspondence should be addressed. blackwell@chem.wisc.edu.

Peptoids, or *N*-substituted glycines, are a class of foldamers that have shown extraordinary promise since their inception nearly two decades ago as part of drug discovery efforts (Figure 1A).[4] The breadth of peptoid function continues to expand,[5] highlighted by recent investigations that have yielded potent antimicrobial agents,[6,7] modulators of protein-protein interactions,[8-11] RNA-binding agents,[12-15] lung surfactants,[16,17] anti-biofouling agents,[18] asymmetric catalysts,[19] and self-assembled nano-structures.[20,21] Peptoids can be synthesized in a straightforward modular fashion[22] and possess desirable characteristics such as proteolytic stability[23] and increased cellular permeability relative to their α-peptide equivalents.[24,25] These attributes make them highly attractive scaffolds for multivalent ligand display[13,26,27] and as potential therapeutic agents.[28] While certain recent studies have revealed that a well-defined structure is not an absolute requirement for biological activity in peptoids,[11] there remains a persistent need to delineate peptoid sequence-structure relationships in order to create well-folded, three-dimensional biomimetic structures.

Initial research on peptoid structure focused primarily on peptoids containing sterically-bulky α-chiral side chains (Figure 1B). In these early studies, molecular modeling experiments predicted that peptoid oligomers comprised of α-chiral aromatic (*S*)-*N*-(1-phenylethyl)glycine (*N*spe) residues would adopt an all *cis*-amide helix with approximately three residues per turn and dihedral angles similar to that of a polyproline type I (PPI) peptide helix.[29] The peptoid helical sense was hypothesized to be dictated by the stereochemistry of the α-chiral side chain, with (*R*) or (*S*) stereocenters producing a left- or right-handed helix, respectively. These modeling studies were later supported by 2D-NMR and X-ray crystallographic experiments. In a 2D-NMR study in methanol, the major conformer of a peptoid pentamer containing five *para*-substituted *N*spe residues was found to adopt an all *cis*-amide, right-handed helix with three residues per turn and a pitch of ~6 Å, analogous to a PPI helix.[30] Interestingly, the CD spectrum of this peptoid pentamer in methanol resembled that of an α-helix, as opposed to a PPI helix, with minima near 220 nm and near 205 nm. It is important to note, however, that the major NMR conformer of the *N*spe pentamer only represented 50–60% of the total molecules in solution due to *cis/trans* isomerization of the backbone tertiary amides, and the *N*spe pentamer CD spectrum was weak relative to longer *N*spe peptoids.[30] This suggested that while the *N*spe pentamer can sample a helical conformation, it was conformationally heterogeneous.

Subsequent investigations of *N*rpe (the *R* variant of *N*spe) peptoid oligomers by Barron and co-workers detailed specific sequence requirements for peptoid helix formation. In these studies, peptoid helicity was promoted in sequences that contained at least 50% α-chiral residues, or α-chiral aromatic side chains every third residue (*i, i*+3 positions), and an α-chiral residue at the C-terminus.[31] Additionally, increasing the oligomer length resulted in peptoids with greater helical character.[32] It would be desirable, however, if fewer than 50% helix-inducing residues were needed to promote a stable and predictable secondary structure. Additional structural diversity could then be installed onto the peptoid backbone relative to *N*spe helices, and this enhancement in structural tunability would be a significant advance for the design of biologically active peptoid helices.

In addition to *N*spe-type oligomers, peptoids with α-chiral aliphatic side chains can also adopt helical structures. X-ray crystallographic analysis of an (*R*)-*N*-(1-cyclohexylethyl)glycine (*N*rch, Figure 1B) pentamer revealed an all *cis*-amide left-handed helix with approximately three residues per turn and a helical pitch of approximately 6.7 Å.[33] The dihedral angles observed in the solid-state structure of this peptoid pentamer were similar to those observed in PPI peptide helices, and were comparable to those observed for the solution-structure of the *para*-substituted *N*spe pentamer introduced above. The CD spectra of the *N*rch pentamer in acetonitrile, in contrast to the *N*spe pentamer, displayed a similar shape to that seen for a PPI peptide helix, with a maxima near 210 nm and two

shallow minima near 200 nm and near 225 nm.[33] Although the X-ray crystallographic data demonstrated that the Nrch pentamer had a helical structure in the solid state, this peptoid, similar to the Nspe pentamer above, was conformationally heterogeneous in solution, as exhibited by its low overall amide $K_{cis/trans}$ value (~1) in acetonitrile (determined by 2D-NMR spectroscopy) and weak CD spectrum.

The previous studies outlined above indicate that the generation of robust, conformationally homogeneous peptoid helices remains a challenge. A more complete understanding of sequence-structure relationships in peptoids would undoubtedly improve the design of well-defined peptoid helices *a priori*, and further expand their utility as biomimetic agents capable of performing specific functions. As highlighted above, *cis/trans* isomerization of the tertiary backbone amides is a major contributor to the conformational heterogeneity observed in many peptoid oligomers.[30] Strategies aimed at enforcing either *cis*- or *trans*-amides within peptoid backbones have continued to evolve as a more thorough understanding of the noncovalent forces affecting peptoid tertiary amide *cis/trans* equilibria have emerged.[34,35] Until recently, the highest reported overall backbone amide $K_{cis/trans}$ value for a peptoid was only approximately 3.2, and this was adopted by $(N$spe$)_{15}$.[32] We have since discovered that the α-chiral aromatic side chain *1npe* (Figure 1B) is highly effective for exclusively promoting the *cis*-amide rotamer within a peptoid backbone, primarily due to steric interactions.[35] NMR analysis of a model peptoid monomer containing this side chain revealed that stereoelectronic effects, namely an n→π*$_{aromatic}$ interaction between the backbone carbonyl oxygen and side chain naphthalene group, could also play a role in stabilizing the *cis*-amide rotamer. 2D-NMR analysis of an Ns1npe trimer, Ac-($s1npe$)$_3$-CONH$_2$, revealed that this oligomer had an overall backbone amide $K_{cis/trans}$ of 9.7 in acetonitrile, which represented the highest reported value for any peptoid oligomer to date.[35] The CD spectrum of Ac-($s1npe$)$_3$-CONH$_2$ showed an intense maximum near 205 nm and an intense minimum near 220 nm, with a magnitude nearly twice that of Nspe$_5$. These exciting initial results suggested that peptoid oligomers comprised of the *1npe* side chain could potentially form well-folded PPI peptoid helices with unprecedented conformational homogeneity in solution.

Herein, we report our efforts toward the generation of well-defined peptoid helices through the systematic design, synthesis, and structural characterization of a series of peptoid homooligomers (1–13-mers) containing the *s1npe* side chain. X-ray crystallographic analysis revealed that an Ns1npe monomer, dimer, trimer, and tetramer each adopt solid-state structures with dihedral angles similar to a PPI peptide helix. 2D-NMR spectroscopic studies showed that these Ns1npe peptoids exhibited very high overall amide $K_{cis/trans}$ values, and CD studies revealed intense and thermally-stable CD spectra, both indicative of exceptionally well-folded structures. The Ns1npe helix represents, to our knowledge, the most conformationally homogeneous peptoid helix reported to date. We anticipate that the ability to generate such well-folded peptoid helices will provide exciting opportunities for the exploration of structure-function relationships in polypeptoids in the future.

Experimental Section

General

All reagents were purchased from commercial sources (Aldrich and Acros) and used without further purification. Solvents were purchased from commercial sources (Aldrich and Fischer) and used as is, with the exception of dichloromethane (CH$_2$Cl$_2$) and *n*-hexane, which were distilled immediately prior to use. Thin layer chromatography (TLC) was performed on silica gel 60 F$_{254}$ plates (E-5715-7, EMD). SiliaFlash P60 silica gel (40–63 μm, Silicycle) was used for manual flash column chromatography.[36]

^{1}H NMR (300 MHz) and ^{13}C NMR (75 MHz) spectra were recorded on either a Bruker AC-300 or a Varian MercuryPlus 300 spectrometer in deuterated solvents. Chemical shifts are reported in parts per million (ppm, δ) using tetramethyl silane (TMS) as a reference (0.0 ppm), unless otherwise noted. Couplings are reported in hertz. Gradient correlation spectroscopy (gCOSY) and heteronuclear single quantum coherence adiabatic (HSQCAD) NMR experiments were performed on either a Varian Inova 500 or 600 MHz spectrometer and were referenced to solvent. The data were processed using the Varian VNMR software package (v. 6.1C) and visualized using SPARKY software.[37]

Matrix-assisted laser desorption/ionization time-of-flight (MALDI-TOF) mass spectra were obtained on a Bruker RELEX II spectrometer equipped with a 337 nm laser and a reflectron. In positive ion mode, the acceleration voltage was 25 kV.

Reversed-phase high performance liquid chromatography (RP-HPLC) was performed using a Shimadzu system equipped with an SCL-10Avp controller, an LC-10AT pump, an FCV-10ALvp solvent mixer, and an SPD-10MAvp UV/vis diode array detector. All analytical RP-HPLC work was performed using either a Restek Premier C18 column (5 μm, 4.6 mm × 250 mm) or a Restek C4 column (5 μm, 4.6 mm × 250 mm). Standard RP-HPLC conditions were as follows: flow rate = 1 mL/min; mobile phase A = 0.1% trifluoroacetic acid (TFA) in water; mobile phase B = 0.1% TFA in acetonitrile. Purities were determined by integration of peaks with UV detection at 220 nm.

LC-MS data were obtained using a Shimadzu LCMS-2010 system equipped with two LC-10ADvp pumps, SCL-10Avp controller, SIL-10ADvp autoinjector, SPD-M10Avp UV/vis diode array detector, and single quadrupole analyzer (by ESI). A Supelco C18 wide-pore column (15 cm × 2.1 mm) was used for all LC-MS work. Standard RP-HPLC conditions for LC-MS were as follows: flow rate = 200 μL/min; mobile phase A = 0.1% formic acid in water; mobile phase B = 0.1% formic acid in acetonitrile.

Attenuated total reflectance (ATR)-IR spectra were recorded with a Bruker Tensor 27 spectrometer, outfitted with a single reflection MIRacle Horizontal ATR and a Ge crystal with a spectral range of 5500 to 700 cm^{-1}. Circular Dichroism (CD) spectra were obtained on an Aviv 62A DS spectropolarimeter with Aviv CDS software.

Synthesis and Characterization of Peptoid Oligomers

Peptoid **1′** was synthesized using microwave-assisted solid-phase methods on Rink-amide-derivatized polystyrene resin as previously reported.[38,39] The crude peptoid was purified by preparative RP-HPLC and characterized by MS to confirm identity (See Table 1). Peptoids **1**–**13** were synthesized in solution using modified versions of previously reported procedures.[40] The crude peptoids were purified by flash silica gel column chromatography and characterized by MS to confirm their identity (See Table 1). See Supporting Information for detailed synthetic procedures and complete compound characterization, including HPLC and MS data, for peptoids **1**–**13** and their respective synthetic intermediates.

NMR Analysis for Peptoid 1 and 1′

Peptoid **1** and **1′** were dissolved in CD_3CN to give a 10 mM solution. ^{1}H NMR spectra were acquired using 16 scans and a relaxation delay of 15 s. 1D-NOESY spectra were acquired to verify previously reported guidelines for distinguishing *cis-* and *trans*-amide rotamers.[41] The K$_{cis/trans}$ ratio was calculated by averaging the integration ratios for three sets of rotamer-related peaks.

NMR Analyses for Peptoid Oligomers 2–13

Peptoids **2**–**13** were dissolved in CD_3CN to give 10 mM solutions and analyzed by gCOSY and HSQCAD NMR experiments as detailed below. The experiments were performed on either a Varian Inova 500 or 600 MHz spectrometer using a 5mm hcn probe. The gCOSY NMR spectra were used for assignment purposes, and the HSQCAD NMR spectra were subsequently integrated to give the $K_{cis/trans}$ values in Table 4. Assignments of methine *cis* and *trans* peaks were based on previously observed trends in chemical shifts.[41]

gCOSY NMR experiments were performed for peptoids **2**–**13** at 24 °C using the following parameter values: Spectral widths were: 5252, 5571, 4667, 4783, 5561, 5804, 5533, 5504, 5513, 5697, 5388, 5320, 3938, and 4139 Hz, respectively. The number of transients (nt) was 8. The relaxation delays (d1) were 4.2, 4.2, 4.2, 4.2, 4.2, 5.9, 4.2, 3.4, 4.2, 4.2, 4.2, 4.2, 4.2, and 2.4, respectively. The number of increments (ni) were 350, 450, 400, 400, 450, 450, 500, 450, 500, 475, 450, 475, 400, and 350, respectively. The number of points was 2048. The spectra were zero-filled to generate matrices of 4096 × 4096 points.

HSQCAD NMR experiments[42] were performed for peptoids **2**–**13** at 24 °C using the following parameter values: Spectral widths were: 5252, 5571, 4667, 4783, 5561, 5804, 5533, 5504, 5513, 5697, 5388, 5320, 3938, and 4139 Hz, respectively, in the ^1H dimension. Spectral widths were 32428, 28582, 23509, 23795, 27972, 26464, 22844, 22792, 22008, 18286, and 19048 Hz, respectively, in the ^{13}C dimension. The relaxation delays (d1) were 2.8, 3, 2.8, 3, 2.8, 3.9, 2.8, 2.8, 3, 2.8, 2.8, 3, 2.8, and 2, respectively. The number of transients (nt) were 6, 8, 6, 6, 6, 8, 8, 6, 8, 8, 8, 12, 8, and 6, respectively. The number of increments (ni) were 260, 256, 300, 300, 250, 250, 250, 250, 256, 250, 256, 256, 250, and 250, respectively. The number of points was 2048. The spectra were zero-filled to generate f1 × f2 matrices of 4096 × 4096 points.

CD Analyses for Peptoids 1–13

Peptoid stock solutions were prepared by dissolving at least 2 mg of each peptoid in spectroscopic grade acetonitrile or methanol. The stock solutions then were diluted with spectroscopic grade solvent to the desired concentration (~60 μM) by mass using a high-precision balance (Mettler-Toledo XS105). CD spectra were obtained in a square quartz cell (path length 0.1 cm) at 24 °C using a scan rate of 100 nm/min. The spectrum of a solvent blank was subtracted from the raw CD data, and the resulting data were expressed in terms of per-residue molar ellipticity (deg cm^2/dmol), as calculated per mole of amide groups present and normalized by the molar concentration of peptoid.

X-ray Crystal Structure Data for 1′ and 2–4

A ~10 mg sample was dissolved in HPLC-grade MeOH (**1′** and **2**), HPLC-grade acetone (**3**), or *n*-hexane in a minimal amount of CH_2Cl_2 (**4**). Slow evaporation at room temperature afforded crystals suitable for X-ray analysis after approximately one week. The X-ray crystal data for **1′** and **2**–**4** have been deposited at the Cambridge Crystallographic Data Centre with deposition numbers 787850–797853. See Supporting Information for complete crystallographic details.

Results and Discussion

Design of Peptoid Oligomers

We sought to investigate the helix-forming propensity of *N*s1npe peptoids relative to previous studies of helical peptoids. As outlined above, these past investigations have used CD and NMR spectroscopy as primary methods to determine overall peptoid helical character. In one prominent study, Barron and co-workers synthesized a series of *N*rpe

homooligomers with lengths varying from 1–20 residues and utilized CD spectroscopy to probe the effects of chain length on peptoid secondary structure.[32] They found that these α-chiral aromatic side chain-containing peptoids adopted largely helical structures in acetonitrile (with few exceptions), and that the degree of helicity became length-independent after 12 residues. In order to compare to this past work, we chose to synthesize a series of peptoid Ns1npe homooligomers with lengths varying from 1–13 residues (Table 1). We hypothesized that these peptoids would also adopt helical conformations in acetonitrile, and that their CD signatures would display a similar length-dependent increase. Moreover, we reasoned that the Ns1npe peptoids would exhibit significantly higher overall amide $K_{cis/trans}$ values relative to Nrpe systems, based on our previously reported $K_{cis/trans}$ values for an Ns1npe monomer (6.3), homodimer (7.0), and homotrimer (9.7).[35]

Synthesis of Peptoid Oligomers

Peptoid oligomers are typically synthesized on solid-phase resins using the highly efficient sub-monomer approach.[22] Using this method for the synthesis of Ns1npe peptoids, however, resulted in low yields and purities of the desired peptoid oligomers after the trimer stage, presumably due to the increased steric congestion of the $s1npe$ side chain. We therefore utilized solution-phase synthetic techniques to generate the peptoid oligomers, and used methods that were similar to previously reported peptoid syntheses (see Supporting Information for details).[34,40] Because such synthetic routes afford the opportunity to install unique functionalities at the C- and N-termini, we selected C- and N-terminal moieties that would be compatible with our investigations into peptoid helix formation and obviate problems of residual functionality associated with solid-phase synthesis. Most peptoid oligomers synthesized on solid-phase resins are cleaved from Rink-amide linkers under TFA-mediated conditions, affording a peptoid with a primary amide at the C-terminus and an ammonium group at the N-terminus. Notably, these functional groups can strongly influence peptoid secondary structure. Hydrogen-bonding interactions between these two termini and multiple carbonyl oxygens within the peptoid backbone play a significant role in stabilizing a competing threaded loop structure at an oligomer length of nine residues, and thereby disfavoring PPI helix formation.[38,41] Additionally, hydrogen-bonding interactions from carbonyl oxygens within the peptoid backbone to the C-terminal amide hydrogens are believed to contribute to conformational heterogeneity in peptoid helices by favoring the presence of *trans*-amide bonds.[30] These problems were avoided by using our solution-phase synthetic approach. While solution-phase synthesis is comparatively more labor-intensive than a solid-phase approach, we were able to reproducibly obtain 50–100 mg of each peptoid oligomer, which proved especially useful for performing a variety of structural experiments on each compound.

We synthesized a series of peptoid Ns1npe homooligomers with lengths varying from 1–13 residues (**1–13**, Table 1) with *t*-butyl esters at the C-termini and acetyl groups at the N-termini to mitigate hydrogen-bonding interactions. We found that the presence of the *t*-butyl ester moiety was adventitious, as it greatly facilitated the crystallization of Ns1npe peptoid dimer, trimer, and tetramer (**2–4**) relative to their respective C-terminal primary amide equivalents. Peptoid monomer **1** did not crystallize despite several attempts, and we therefore include **1′** for crystallographic analysis purposes. The Nspe pentamer **5′**, which contains an acetylated N-terminus and a *t*-butyl ester at the C-terminus, was also synthesized as a key control to allow for spectroscopic comparison to previously reported Nspe peptoids.

X-ray Crystallographic Study of N1npe oligomers

Peptoids **1′** and **2–4** readily crystallized, and we analyzed their solid-state structures by X-ray crystallography (Figure 2). The backbone amide bonds in each peptoid all adopted *cis*-amide conformations. Notably, the X-ray crystal structure of tetramer **4** revealed that this

oligomer adopted a right-handed nascent helix with approximately three residues per turn and a helical pitch of approximately 6.0 Å. This structure is significant, as it represents the first reported X-ray crystal structure of a peptoid with α-chiral aromatic side chains. Analysis of the structures of **1′**, **2**, and **3** shows the gradual progression of helix formation seen in tetramer **4** (Figure 2). The pitch observed in the solid-state structure of **4** is in agreement with the pitch of ~6 Å previously reported for a *para*-substituted *N*spe pentamer, as experimentally determined by 2D-NMR spectroscopy in methanol (see above).[30] These pitch distances deviate slightly from the pitch of ~6.7 Å observed in the solid-state structure of the related, aliphatic *N*rch pentamer.[33] A possible reason for this difference could be the smaller steric size of the *N*s1npe planar aromatic rings relative to the *N*rch cyclohexyl ring, which may allow the helix to compress into a more compact conformation.

The ϕ and ψ backbone dihedral angles of peptoid **1′** and **2**–**4** are listed in Table 3. Interestingly, at least one ω (amide) dihedral angle in each peptoid deviates significantly from planarity, ranging in value from −20° to 8° (equivalent to 340° to 8°). Non-planar amides have previously been observed previously in the X-ray crystal structures of certain macrocyclic peptoids.[43] In these compounds, steric interactions upon macrocycle formation have been hypothesized to lower the energetic barrier to amide bond rotation and thus contribute to the amide bond distortion. Steric interactions between amide side chains also could be a cause for the observed amide distortions in **1′** and **2**–**4**.

We also note that none of the naphthalene groups in these four solid-state structures are oriented in such a way as to facilitate an n→π*_aromatic backbone to side chain interaction. This is in contrast to our understanding of the noncovalent interactions involved in stabilizing *cis*-amides in *N*s1npe systems in solution, ascertained from our earlier NMR studies of a model *N*s1npe-type monomer (see above).[35] However, crystal lattice interactions within these peptoids may provide an explanation. Views of the solid-state packing of peptoids **1′** and **2**–**4** are provided in the Supporting Information (Figures S-7–S-11). These structures show that the side chain naphthalene groups of adjacent peptoids are in close contact with one another, and are aligned in orientations that allow for tight crystal packing. These packing interactions may be preventing the peptoids from crystallizing with the naphthalene groups involved in an intraresidue n→π*_aromatic interaction. Importantly, we did not observe any specific, non-covalent intermolecular interactions in the solid-state that impacted the backbone dihedral angles for **1′** and **2**–**4**, and therefore the progressive formation of PPI peptoid structure is maintained in all four solid-state structures.

2D-NMR studies

We sought to examine the solution-phase conformations of peptoids **1**–**13**, and utilized ^{1}H gCOSY and ^{1}H-^{13}C HSQCAD NMR experiments to determine overall backbone amide K_{cis/trans} values in acetonitrile. These 2D-NMR experiments are typically used to determine the presence of different conformational isomers of peptoids in solution.[31,33,38] In the case of PPI peptoid helices, a peptoid oligomer that exhibits a high overall backbone amide K_{cis/trans} value is more conformationally homogeneous relative to a peptoid oligomer with a low K_{cis/trans} value. We were pleased to observe extremely high K_{cis/trans} values (4.9 to >19) for all of the *N*s1npe peptoids (**1**–**13**; Table 4). These values increase in a length-dependent fashion, with *trans*-amide conformations becoming virtually undetectable at the tetramer (**4**) stage and beyond. To our knowledge, the overall backbone amide K_{cis/trans} value of 19 for *N*s1npe peptoids **4**–**13** are the highest reported for any peptoid oligomer to date.

To compare our *N*s1npe systems to previously reported *N*spe peptoids, we examined the K_{cis/trans} values of the *N*s1npe pentamer **5** and the *N*spe pentamer **5′**. These values were >19 and 3.3, respectively. A direct comparison to past reports is not possible, as these *N*spe-type peptoids had different functionality at the N- and C-termini. However, the striking

difference in K*cis/trans* between these two pentamers suggests that *N*s1npe **5** is considerably more conformationally homogeneous than *N*spe **5′** in acetonitrile. We also observed that the distribution of *cis*-amide methine peaks in the HSQC spectra of *N*s1npe peptoids gradually narrowed as oligomer length increased from 1–13 residues (See Supporting Information). This reduction in the number of peaks in the HSQC NMR spectra and a corresponding increase in CD signal intensity (see below) is indicative of an increasingly ordered structure.[33] The reasons for this enhanced helix stability relative to *N*spe systems could be multifold, but we believe that steric interactions between the bulky naphthalene-containing side chains play an essential role. Additional spectroscopic and computational experiments are necessary to further understand such interactions and other related phenomena, and are ongoing.

CD Analysis of Peptoid Oligomers

We utilized CD spectroscopy to further analyze the conformations of peptoids **1**–**13** in solution. The CD spectra of peptoids **1**–**13** and **5′** in acetonitrile at room temperature are shown in Figures 3-5. Peptoids **1**–**3** had similar CD spectra, with intense minima near 220 nm and intense maxima near 205 nm (Figure 3). These CD spectra were analogous in shape and intensity to the CD spectra that we had previously reported for their primary amide analogs Ac-(*s1npe*)$_1$-CONH$_2$ (**1′**), Ac-(*s1npe*)$_2$-CONH$_2$, and Ac-(*s1npe*)$_3$-CONH$_2$, respectively.[35] Intriguingly, the CD spectrum of tetramer **4** had a different spectral shape than peptoids **1**–**3**. This spectrum had a reduced minimum near 220 nm, and an increased maximum near 205 nm, along with the concomitant appearance of a new and intense minimum near 230 nm. We note that tetramer **4** represents the first possible oligomer in the series in which *s1npe* side chains could spatially overlap in one turn of a helix, as indicated in the X-ray crystal structure of tetramer **4** (Figure 2). This $i \rightarrow i\pm3$ overlap of the napthyl side chains could contribute to the different CD spectral shapes observed for tetramer **4** relative to the shorter peptoids **1**–**3**.

The CD spectrum of tetramer **4** was then compared to the spectra obtained for peptoids **5**–**8** and **5′** (Figure 4). Peptoids **5**–**8** each have a spectral shape similar to tetramer **4** with intense minima near 230 nm, shallow minima at 220 nm that decrease in intensity with increasing chain length, and broad maxima near 205 nm. The intensities of the minima near 230 nm increase with oligomer length, with peptoids **7** and **8** displaying nearly identical intensities. Overall, the length-dependent increase in ellipticity per amide in the CD spectra of peptoids **1**–**8** suggests that helix folding could be a cooperative process,[32,44] despite the lack of any apparent long-range noncovalent interactions. It is reasonable to suggest that the formation of *N*1npe secondary structure could arise, in part, from the ability of the bulky *N*1npe residues to sterically exclude space for adjacent residues to sample. However, longer oligomers have a greater internal- to end-residue ratio compared to shorter oligomers, and we cannot discount that this ratio also contributes to the observed length dependent intensity of the CD data for peptoids **1**–**8**. Further experiments, including thermal denaturation studies, are necessary to explore these phenomena, and are ongoing.

As mentioned above, the CD spectrum of an *N*spe pentamer in methanol resembles that of an α-helix,[30] while polypeptoids containing *N*rch (and related) residues display a distinct maximum at 210 nm and two shallow minima at 195 and 225 nm in their CD spectra,[33] which is characteristic of a PPI helix. We observed that the CD spectrum for *N*spe pentamer **5′** in acetonitrile (Figure 4) showed a weak α-helical signature with two minima at 202 nm and 220 nm, which matches previously reported CD spectra of peptoids containing this same α-chiral and aromatic side chain, but was completely different from the spectrum of *N*s1npe pentamer **5**. Indeed, the unique CD spectra observed for *N*s1npe peptoids in this study provide further supporting evidence that the CD spectral shape of similar peptoid structures can vary greatly depending on the identity of the side chains within the peptoid oligomer.

We note, however, that *N*s1npe, *N*spe, and *N*rch peptoids also have varying degrees of conformational homogeneity, and this could alter their CD spectra as well.

Continuing in the length-dependent series, peptoids **9**–**13** exhibited CD spectra (Figure 5) that were slightly different from the CD spectra of **4**–**8** (Figure 4). The maxima in **9**–**13** increased and were red-shifted from near 205 nm to near 210 nm, and the minima showed a slight red-shifting from near 229 nm to near 231 nm. Intriguingly, the minima near 231 nm in **9**–**13** *decreased* in a length-dependent manner. These results are in contrast to the CD data presented above for **1**–**8** and to previously reported length-dependent CD studies of *N*spe peptoids in which no decrease in CD signal intensity was observed at increasing peptoid oligomer lengths up to 20 residues.[32] An interesting possibility for the observed trend in peptoids **9**–**13** could be the formation of self-associated multimeric structures, which may be affecting the CD signal intensities at these longer chain lengths and may be unique to the *N*1npe primary sequence. However, lowering the concentration to 6 μM did not affect the CD spectral shape or intensity of peptoid **6** or **13** (see Supporting Information). Additional studies are needed to assess the nature and significance of these interactions on the CD signal of *N*s1npe peptoids, if any.[45]

We next obtained variable-temperature CD spectra of the *N*s1npe peptoids to assess their thermal stability, and we selected two peptoids for focused study (**6** and **13**). We chose hexamer **6** because it displayed the most intense minimum (near 229 nm) of any of the peptoids **1**–**13**, and **13** because it represents the longest sequence in the series. The CD spectrum of **6** showed no change in shape and only a moderate decrease in the CD signal intensity over the temperature range 5–75 °C (See Supporting Information). Peptoid **13** also maintained its spectral shape over this temperature range, and displayed only a small reduction in signal intensity (Figure 6). These CD data are in agreement with previous studies on the thermal stability of *N*spe peptoids,[32,44] and demonstrate that the structures of *N*s1npe peptoid oligomers are thermally stable up to 75 °C.

Lastly, we sought to probe solvent effects on the conformations of *N*s1npe peptoids by CD, and selected the polar protic solvent methanol for study. We examined four *N*s1npe polypeptoids of varying lengths from our series (**3**, **6**, **9**, and **12**) by CD in methanol at 24 °C. The CD spectra are shown in Figure 7 and are nearly identical in intensity and shape as to those observed in acetonitrile for these four peptoids (Figures 3-5). These CD data suggest that *N*s1npe polypeptoids can also adopt PPI helices in polar protic solvents. Furthermore, this apparent insensitivity to solvent type supports our hypothesis that steric interactions are a primary cause for conformational restriction in these systems. Maintenance of the *N*s1npe helix in methanol is particularly significant, as it bodes well for the future development of *N*s1npe helices for applications that demand aqueous solubility.

Summary and Outlook

We have discovered that *N*s1npe peptoids can form extraordinarily well-folded PPI helices. X-ray crystallographic studies indicate that an *N*s1npe peptoid monomer, dimer, trimer, and tetramer each adopt structures with all *cis*-amide bonds and dihedral angles similar to those seen in PPI peptide and peptoid helices. The *N*s1npe tetramer (**4**) adopts a right-handed helix in the solid state, and the length-dependent set of *N*s1npe peptoids **1′** and **2**–**4** yielded the first X-ray crystal structures for any peptoid with α-chiral aromatic side chains. 2D-NMR spectroscopic studies revealed that *N*s1npe peptoids **1**–**13** showed very high overall backbone amide $K_{cis/trans}$ values in acetonitrile, consistent with an all *cis*-amide, conformationally homogenous structure. Additionally, peptoids **1**–**13** exhibited intense, length-dependent CD signatures in both acetonitrile and methanol. The 2D-NMR and CD spectroscopic data support the observed solid-state structures of the *N*s1npe monomer, dimer, trimer, and tetramer, and indicate that *N*s1npe peptoids adopt a PPI helix, both in

solution and in the solid state. We anticipate that the ability to generate such well-folded peptoid helices *via* the incorporation of *N*s1npe residues will provide opportunities for the exploration and delineation of new structure-function relationships in peptoids. Most notably, these new structure-promoting elements should prove especially useful for constructing helical peptoid scaffolds with an expanded number of side chain sites available for rational or combinatorial diversification relative to *N*spe heteropeptoids.[31,32] Reducing the number of required hydrophobic peptoid helix-inducing residues from 50% should also promote enhanced water solubilities at longer residue numbers.

In view of the results described here, an exciting prospect for future peptoid design would involve the incorporation of the *cis*-amide-promoting *1npe* side chain in conjunction with the *trans*-amide-promoting *N*-aryl side chain (that we and others have reported)[46,47] into peptoid oligomers. The resulting *cis*- and *trans*-amide residues could be introduced in a variety of different sequence patterns, alternating and otherwise, which could potentially result in the formation of entirely unique secondary structures, and thus expand the known conformational space adopted by peptoids. Ongoing work in our laboratory is directed at utilizing these and other evolving peptoid sequence-structure relationships to design and generate novel polypeptoid architectures.

Supplementary Material

Refer to Web version on PubMed Central for supplementary material.

Acknowledgments

References and Notes

(1). Gellman SH. Acc. Chem. Res. 1998; 31:173–180.

(2). Goodman CM, Choi S, Shandler S, DeGrado WF. Nat. Chem. Biol. 2007; 3:252–262. [PubMed: 17438550]

(3). Yoo B, Kirshenbaum K. Curr. Opin. Chem. Biol. 2008; 12:714–721. [PubMed: 18786652]

(4). Simon RJ, Kania RS, Zuckermann RN, Huebner VD, Jewell DA, Banville S, Ng S, Wang L, Rosenberg S, et al. Proc. Natl. Acad. Sci. U. S. A. 1992; 89:9367–9371. [PubMed: 1409642]

(5). Fowler SA, Blackwell HE. Org. Biomol. Chem. 2009; 7:1508–1524. [PubMed: 19343235]

(6). Chongsiriwatana NP, Patch JA, Czyzewski AM, Dohm MT, Ivankin A, Gidalevitz D, Zuckermann RN, Barron AE. Proc. Natl. Acad. Sci. U. S. A. 2008; 105:2794–2799. [PubMed: 18287037]

(7). Patch JA, Barron AE. J. Am. Chem. Soc. 2003; 125:12092–12093. [PubMed: 14518985]

(8). Simpson LS, Burdine L, Dutta AK, Feranchak AP, Kodadek T. J. Am. Chem. Soc. 2009; 131:5760–5762. [PubMed: 19351156]

(9). Udugamasooriya DG, Dineen SP, Brekken RA, Kodadek T. J. Am. Chem. Soc. 2008; 130:5744–5752. [PubMed: 18386897]

(10). Lim H-S, Archer CT, Kodadek T. J. Am. Chem. Soc. 2007; 129:7750–7751. [PubMed: 17536803]

(11). Hara T, Durell SR, Myers MC, Appella DH. J. Am. Chem. Soc. 2006; 128:1995–2004. [PubMed: 16464101]

(12). Lee MM, Pushechnikov A, Disney MD. ACS Chem. Biol. 2009; 4:345–355. [PubMed: 19348464]

(13). Lee MM, Childs-Disney JL, Pushechnikov A, French JM, Sobczak K, Thornton CA, Disney MD. J. Am. Chem. Soc. 2009; 131:17464–17472. [PubMed: 19904940]

(14). Labuda LP, Pushechnikov A, Disney MD. ACS Chem. Biol. 2009; 4:299–307. [PubMed: 19278238]

(15). Chirayil S, Chirayil R, Luebke KJ. Nucleic Acids Res. 2009; 37:5486–5497. [PubMed: 19561197]

(16). Seurynck-Servoss SL, Dohm MT, Barron AE. Biochemistry. 2006; 45:11809–11818. [PubMed: 17002281]

(17). Brown NJ, Wu CW, Seurynck-Servoss SL, Barron AE. Biochemistry. 2008; 47:1808–1818. [PubMed: 18197709]

(18). Statz AR, Meagher RJ, Barron AE, Messersmith PB. J. Am. Chem. Soc. 2005; 127:7972–7973. [PubMed: 15926795]

(19). Maayan G, Ward MD, Kirshenbaum K. Proc. Natl. Acad. Sci. U. S. A. 2009; 106:13679–13684. [PubMed: 19667204]

(20). Nam KT, Shelby SA, Choi PH, Marciel AB, Chen R, Tan L, Chu TK, Mesch RA, Lee B-C, Connolly MD, Kisielowski C, Zuckermann RN. Nat. Mater. 2010; 9:454–460. [PubMed: 20383129]

(21). Murnen HK, Rosales AM, Jaworsk JN, Segalman RA, Zuckermann RN. J. Am. Chem. Soc. 2010; 132:16112–16119. [PubMed: 20964429]

(22). Zuckermann RN, Kerr JM, Kent SBH, Moos WH. J. Am. Chem. Soc. 1992; 114:10646–10647.

(23). Miller SM, Simon RJ, Ng S, Zuckermann RN, Kerr JM, Moos WH. Bioorg. Med. Chem. Lett. 1994; 4:2657–2662.

(24). Tan NC, Yu P, Kwon Y-U, Kodadek T. Bioorg. Med. Chem. 2008; 16:5853–5861. [PubMed: 18490170]

(25). Kwon Y-U, Kodadek T. J. Am. Chem. Soc. 2007; 129:1508–1509. [PubMed: 17283989]

(26). Holub JM, Garabedian MJ, Kirshenbaum K. QSAR Comb. Sci. 2007; 26:1175–1180.

(27). Reddy MM, Bachhawat-Sikder K, Kodadek T. Chem. Biol. 2004; 11:1127–1137. [PubMed: 15324814]

(28). Zuckermann RN, Kodadek T. Curr. Opin. Mol. Ther. 2009; 11:299–307. [PubMed: 19479663]

(29). Armand P, Kirshenbaum K, Falicov A, Dunbrack RL Jr. Dill KA, Zuckermann RN, Cohen FE. Folding Des. 1997; 2:369–375.

(30). Armand P, Kirshenbaum K, Goldsmith RA, Farr-Jones S, Barron AE, Truong KTV, Dill KA, Mierke DF, Cohen FE, Zuckermann RN, Bradley EK. Proc. Natl. Acad. Sci. U. S. A. 1998; 95:4309–4314. [PubMed: 9539733]

(31). Wu CW, Sanborn TJ, Huang K, Zuckermann RN, Barron AE. J. Am. Chem. Soc. 2001; 123:6778–6784. [PubMed: 11448181]

(32). Wu CW, Sanborn TJ, Zuckermann RN, Barron AE. J. Am. Chem. Soc. 2001; 123:2958–2963. [PubMed: 11457005]

(33). Wu CW, Kirshenbaum K, Sanborn TJ, Patch JA, Huang K, Dill KA, Zuckermann RN, Barron AE. J. Am. Chem. Soc. 2003; 125:13525–13530. [PubMed: 14583049]

(34). Gorske BC, Bastian BL, Geske GD, Blackwell HE. J. Am. Chem. Soc. 2007; 129:8928–8929. [PubMed: 17608423]

(35). Gorske BC, Stringer JR, Bastian BL, Fowler SA, Blackwell HE. J. Am. Chem. Soc. 2009; 131:16555–16567. [PubMed: 19860427]

(36). Still WC, Kahn M, Mitra A. J. Org. Chem. 1978; 43:2923–2925.

(37). Goddard, TD.; Kneller, DG. SPARKY, v. 3.110. University of California; San Francisco:

(38). Gorske BC, Blackwell HE. J. Am. Chem. Soc. 2006; 128:14378–14387. [PubMed: 17076512]

(39). Gorske BC, Jewell SA, Guerard EJ, Blackwell HE. Org. Lett. 2005; 7:1521–1524. [PubMed: 15816742]

(40). Hjelmgaard T, Faure S, Caumes C, De Santis E, Edwards AA, Taillefumier C. Org. Lett. 2009; 11:4100–4103. [PubMed: 19705862]

(41). Huang K, Wu CW, Sanborn TJ, Patch JA, Kirshenbaum K, Zuckermann RN, Barron AE, Radhakrishnan I. J. Am. Chem. Soc. 2006; 128:1733–1738. [PubMed: 16448149]

(42). Boyer RD, Johnson R, Krishnamurthy K. J. Magn. Reson. 2003; 165:253–259. [PubMed: 14643707]

(43). Shin SBY, Yoo B, Todaro LJ, Kirshenbaum K. J. Am. Chem. Soc. 2007; 129:3218–3225. [PubMed: 17323948]

(44). Kirshenbaum K, Barron AE, Goldsmith RA, Armand P, Bradley EK, Truong KTV, Dill KA, Cohen FE, Zuckermann RN. Proc. Natl. Acad. Sci. U. S. A. 1998; 95:4303–4308. [PubMed: 9539732]

(45). A decrease in CD signal intensity correlating with increasing oligomer length has previously been observed in *N*spe homooligomers; however, these *N*spe peptoids contain termini that can participate in hydrogen bonding, and thus contribute to the formation of *trans*-amide bonds and a corresponding reduced helix character. See reference 41.

(46). Shah NH, Butterfoss GL, Nguyen K, Yoo B, Bonneau R, Rabenstein DL, Kirshenbaum K. J. Am. Chem. Soc. 2008; 130:16622–16632. [PubMed: 19049458]

(47). Stringer JR, Crapster JA, Guzei IA, Blackwell HE. J. Org. Chem. 2010; 75:6068–6078. [PubMed: 20722367]
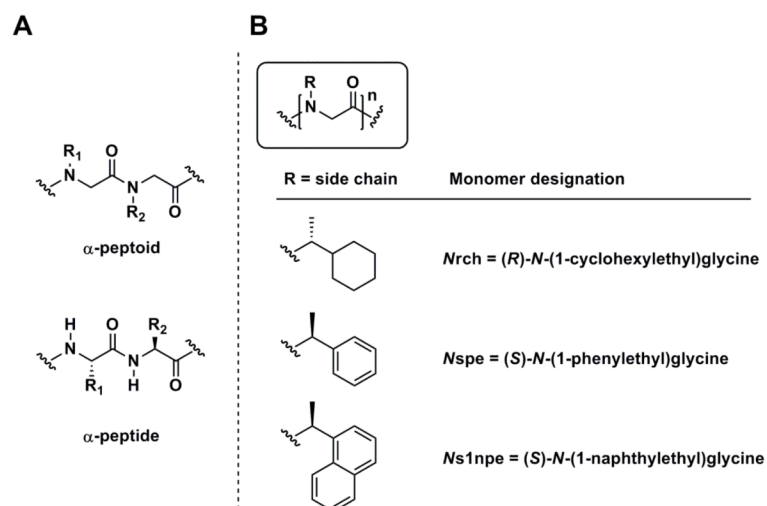
Figure 1.
(A) Comparison of the primary structures of an α-peptoid to an α-peptide. (B) *N*-substituted glycine side chains discussed in this study.
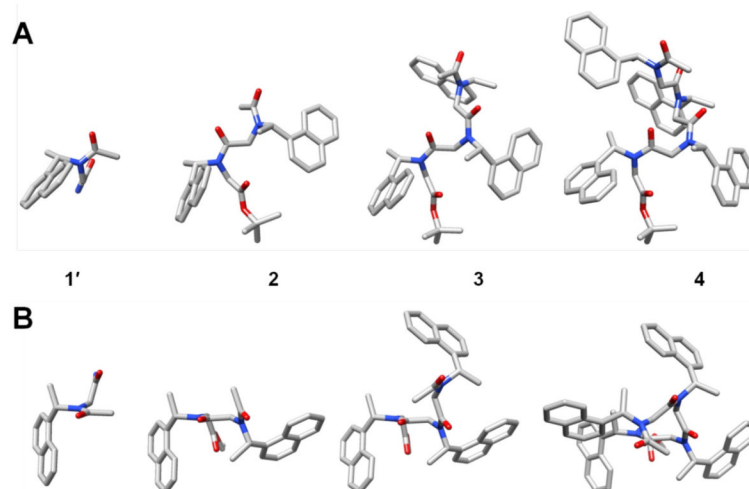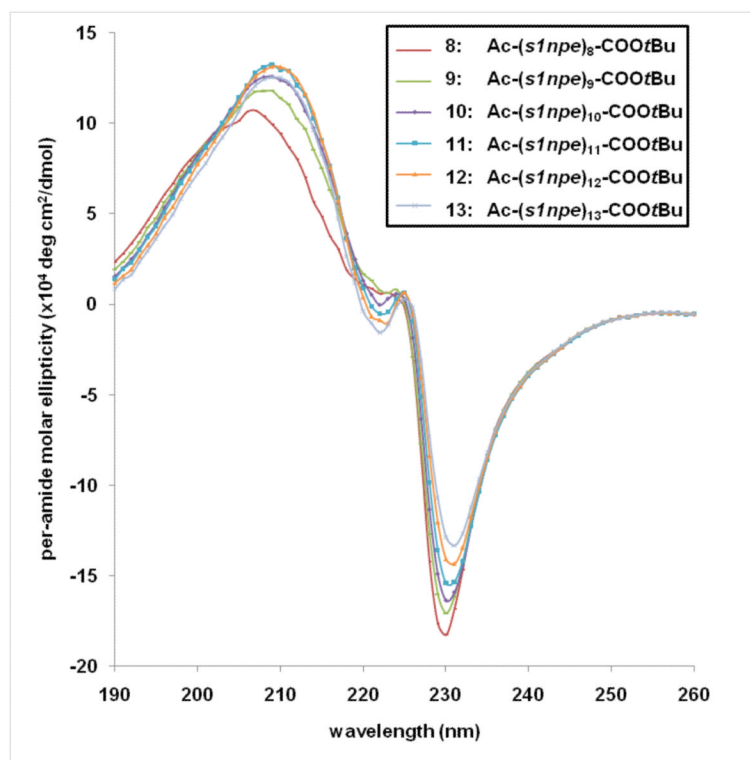
Figure 2.
X-ray crystal structures of peptoids **1′** and **2**–**4**. (A) View perpendicular to the helical axis. (B) View parallel to the helical axis. Atom designations: red = oxygen; blue = nitrogen; gray = carbon. Hydrogen atoms in (A) and (B) and the *t*-butyl methyl groups in (B) have been removed for clarity.
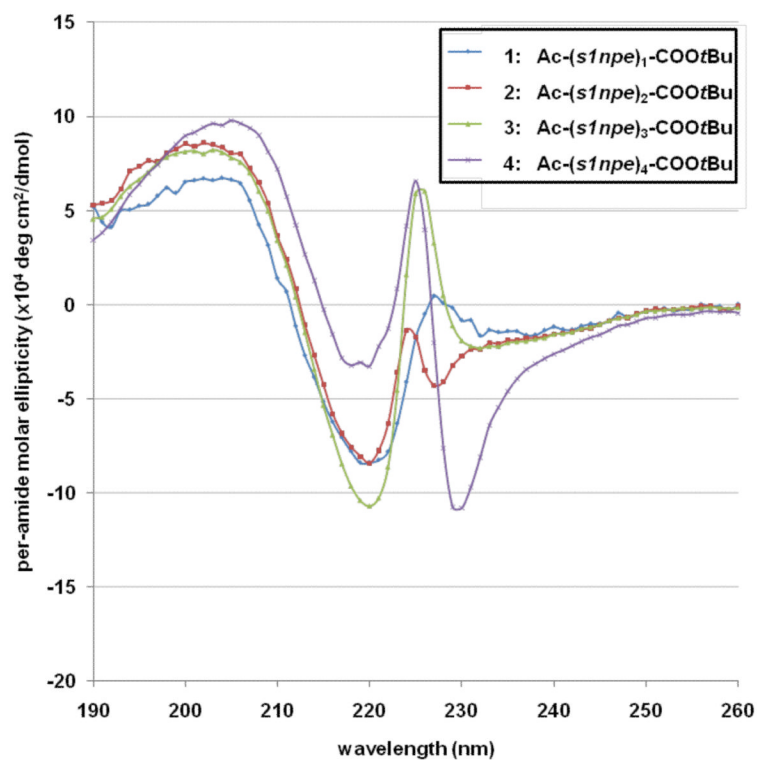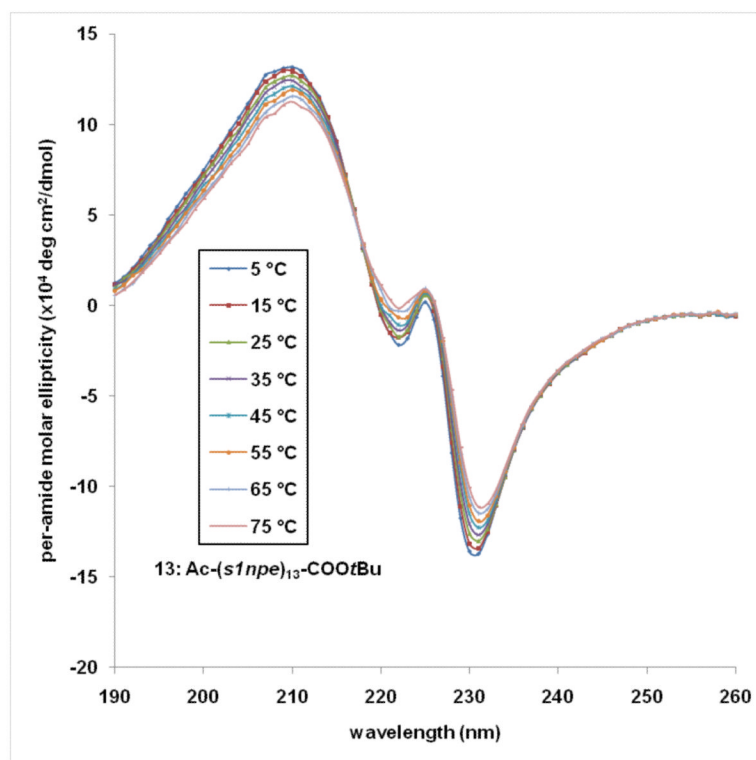
Figure 3.
CD spectra of peptoids **1**–**4** at ~60 μM in acetonitrile. Spectra were collected at 24 °C.
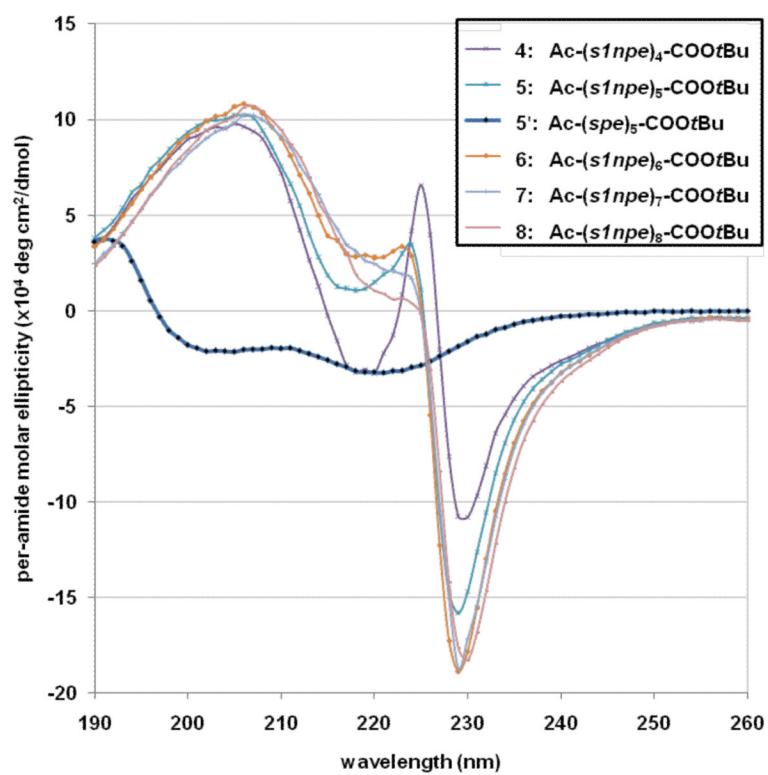
Figure 4.
CD spectra of peptoids **4–8** and **5′** at ~60 μM in acetonitrile. Spectra were collected at 24 °C.

Figure 5.
CD spectra of peptoids **8**–**13** at ~60 μM in acetonitrile. Spectra were collected at 24 °C.

Figure 6.
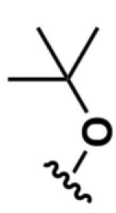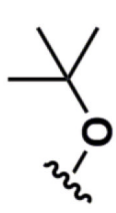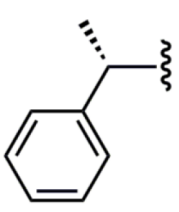CD spectra of peptoid **13** at ~60 μM in acetonitrile. Data were collected between 5–75 °C in 10 ° increments.
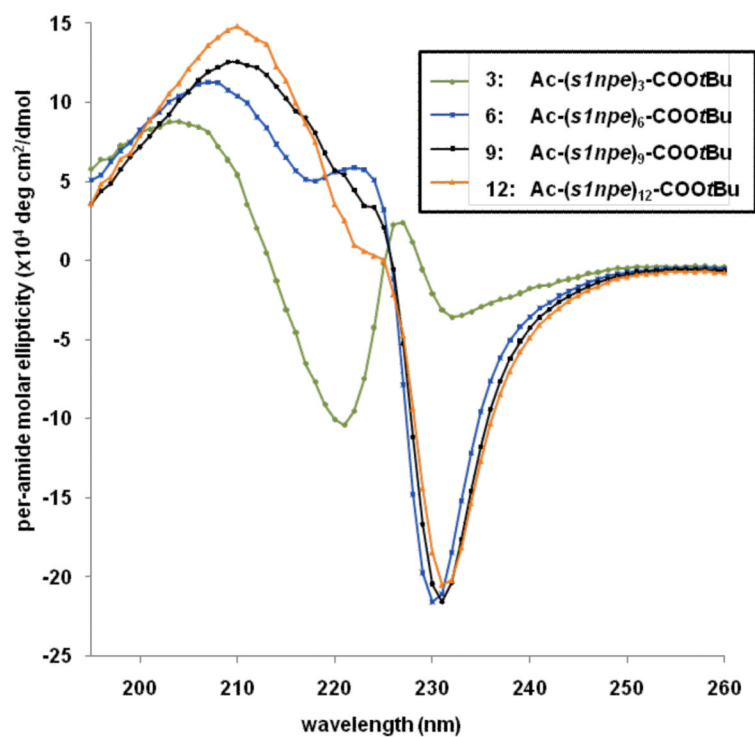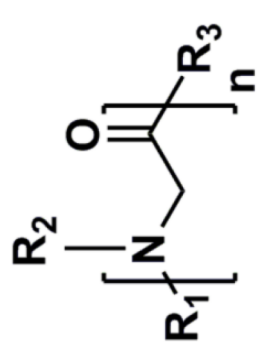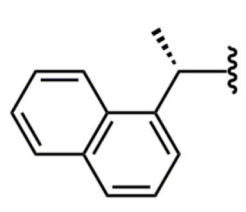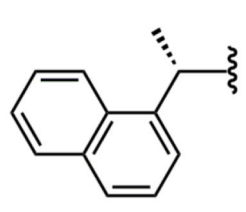
Figure 7.
CD spectra of peptoids **3**, **6**, **9,** and **12** at ~60 μM in methanol. Spectra were collected at 24 °C.

Table 1

Peptoid N-terminal Group, Side Chains, and C-terminal Groups in this Study.

N-substituted glycine, or peptoid

N-terminus – R_1	Side chains – R_2	C-termini – R_3
Ac	s1npe	OtBu
	spe	NH₂

Table 2

Structures, Purities, and Mass Spectral Data for Peptoids **1**–**13**, **1′**, and **5′**.

peptoid	monomer sequence (amino to carboxy terminus)	% purity[a]	calculated mass	observed mass[b]
1	Ac-*s1npe*-COO*t*Bu	99	327.2	328.2 [M+H]+
1′	Ac-*s1npe*-CONH$_2$	99	270.1	293.2 [M+Na]+
2	Ac-(*s1npe*)$_2$-COO*t*Bu	99	538.4	561.2 [M+Na]+
3	Ac-(*s1npe*)$_3$-COO*t*Bu	99	749.4	772.7 [M+Na]+
4	Ac-(*s1npe*)$_4$-COO*t*Bu	98	960.5	984.0 [M+Na]+
5	Ac-(*s1npe*)$_5$-COO*t*Bu	98	1171.7	1195.6 [M+Na]+
5′	Ac-(*spe*)$_5$-COO*t*Bu	99	921.5	944.6 [M+Na]+
6	Ac-(*s1npe*)$_6$-COO*t*Bu	98	1382.7	1406.6 [M+Na]+
7	Ac-(*s1npe*)$_7$-COO*t*Bu	96	1594.8	1617.6 [M+Na]+
8	Ac-(*s1npe*)$_8$-COO*t*Bu	97	1805.9	1828.9 [M+Na]+
9	Ac-(*s1npe*)$_9$-COO*t*Bu	95	2017.0	2039.8 [M+Na]+
10	Ac-(*s1npe*)$_{10}$-COO*t*Bu	98	2228.1	2251.2 [M+Na]+
11	Ac-(*s1npe*)$_{11}$-COO*t*Bu	95	2439.2	2462.3 [M+Na]+
12	Ac-(*s1npe*)$_{12}$-COO*t*Bu	96	2650.3	2673.3 [M+Na]+
13	Ac-(*s1npe*)$_{13}$-COO*t*Bu	95	2862.5	2885.8 [M+Na]+

[a]Determined by integration of the HPLC trace with UV detection at 220 nm.

[b]Mass spectrometry data were acquired using either ESI or MALDI-TOF techniques.

Table 3

Observed Torsion Angles of Peptoids **1'** and **2–4** as Determined by X-ray Crystallography.

peptoid	residue	ω	ϕ	ψ	χ_1
1'	1	−9.4	−79.0	−149.7	−125.7
2	1	−17.1	−68.7	−167.3	−126.7
	2	2.2	82.7	166.0	−135.7
3	1	−13.9	−71.7	−160.6	−136.4
	2	−16.4	−67.8	−163.5	−132.4
	3	8.0	82.8	162.5	−124.6
4	1	3.1	−88.8	−173.7	−83.6
	2	−19.9	−65.3	−178.8	−128.4
	3	−11.7	−66.8	177.2	−120.3
	4	−1.5	75.7	178.3	−149.4

Table 4

Peptoid Structures **1**–**13**, **1′**, and **5′** and Their Respective Overall K$_{cis/trans}$ Values, as determined by ^{1}H-COSY and ^{1}H-^{13}C HSQCAD NMR in CD$_3$CN at 24 °C.

peptoid oligomer	monomer sequence (amino to carboxy terminus)	overall K$_{cis/trans}$[a]
1	Ac-*s1npe*-COO*t*Bu	4.9[b]
1′	Ac-*s1npe*-CONH2	3.8[b]
2	Ac-(*s1npe*)2-COO*t*Bu	10.8
3	Ac-(*s1npe*)3-COO*t*Bu	16.0
4	Ac-(*s1npe*)4-COO*t*Bu	>19
5	Ac-(*s1npe*)5-COO*t*Bu	>19
5′	Ac-(*spe*)5-COO*t*Bu	3.3
6	Ac-(*s1npe*)6-COO*t*Bu	>19
7	Ac-(*s1npe*)7-COO*t*Bu	>19
8	Ac-(*s1npe*)8-COO*t*Bu	>19
9	Ac-(*s1npe*)9-COO*t*Bu	>19
10	Ac-(*s1npe*)10-COO*t*Bu	>19
11	Ac-(*s1npe*)11-COO*t*Bu	>19
12	Ac-(*s1npe*)12-COO*t*Bu	>19
13	Ac-(*s1npe*)13-COO*t*Bu	>19

[a]Weighted average of K$_{cis/trans}$ for all residues.

[b]Determined by integration of 1D-^{1}H NMR spectrum.